UNIVERSITAT DE BARCELONA

Departament d'Astronomia i Meteorologia

Astrophysical Studies on Open Clusters:

NGC 1807, NGC 1817, NGC 2548 and NGC 2682

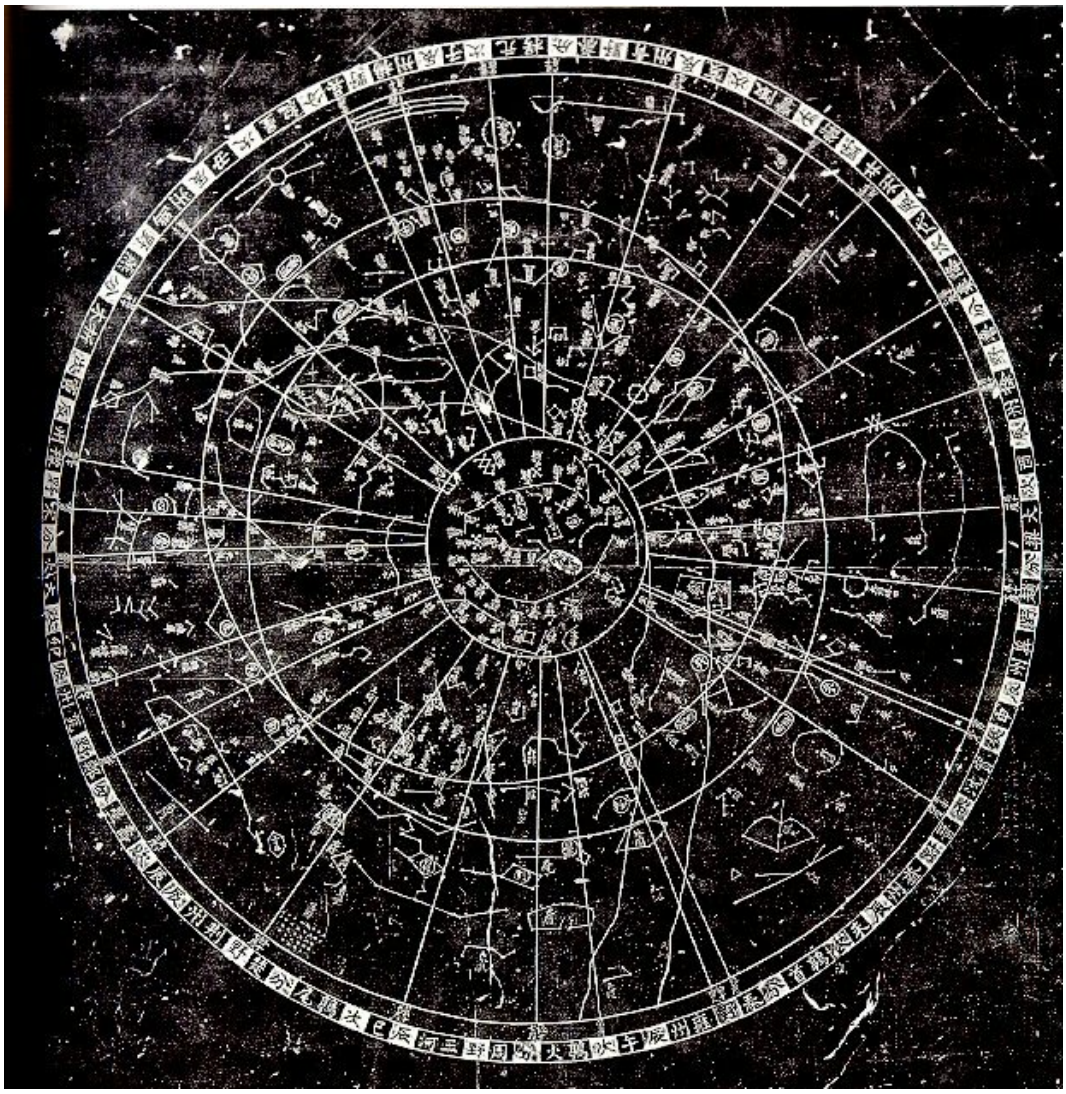

Memoria presentada por

María de los Dolores Balaguer Núñez

para optar al grado de

Doctora en Física

Barcelona, 31 de octubre de 2005

宮詞

玉樓天半起笙歌，
風送宮嬪笑語和。
月殿影開聞夜漏，
水晶簾捲近秋河。

顧況 (725- 814)

A Palace Poem

High above, from a jade chamber, songs float half-way to heaven,
The palace-girls' gay voices are mingled with the wind –
But now they are still, and you hear a clepsydra drip in the Court of the Moon...
They have opened the curtain wide, they are facing the Milky Way.

Gu Kuang (725 - 814)

5 NGC 2548: $uvby - H_\beta$ CCD Photometry and membership segregation

The only existing photometric analysis of NGC 2548 are those of Rider et al. (2004) that gives photometry in the Sloan system with a magnitude limit $g' \sim 18$, and a recent study by Wu et al. (2005) that gives BATC photometry in 13 filters.

In this Chapter[1] we discuss the results of our deep wide-field $uvby - H_\beta$ CCD photometric study of NGC 2548, covering an area of $34' \times 34'$ down to $V \sim 22$.

5.1 The Data

5.1.1 Observations

Deep Strömgren CCD photometry of the area was performed at the Calar Alto Observatory (Almería, Spain) in January 1999 and January 2000 using the 1.23 m telescope of the Centro Astronómico Hispano-Alemán (CAHA) and in January 1999 and February 2000 using the 1.52 m telescope of the Observatorio Astronómico Nacional (OAN). Further data were obtained at the Observatorio del Roque de los Muchachos (ORM, La Palma, Canary Islands, Spain) in February 2000 using the 2.5 m Isaac Newton Telescope (INT) of the ING (equipped with the Wide-Field Camera, WFC), and in December 1998 and February 2000 using the 1 m Jakobus Kapteyn Telescope (JKT) of the ING, with the H_β filter. The poor quality of the images

[1]Based on: Balaguer-Núñez L., Jordi C., & Galadí-Enríquez D., 2005a, A&A 437, 457

Table 5.1: Log of the observations

Telescope	Date	Seeing(″)	n. of frames	Exp. Times (s)				
				u	v	b	y	H_β
1.23 m CAHA	1999/01/12-15	(1)	13	1900	800	400	400	2000
1.23 m CAHA	2000/01/05-10	1.1	21	2200	1400	900	800	1400
1.52 m OAN	1999/01/13-16	(1)	15	1900	800	400	400	2000
1.52 m OAN	2000/02/07-14	(1)	5	-	-	-	-	1400
1 m JKT	1998/12/11-14	(1)	26	2000	1200	800	700	1200
1 m JKT	2000/02/02-06	1.1	18	-	-	-	-	2000
2.5 m WFC-INT	2000/02/02-03	1.3	17	2000	2000	1200	500	-
2.5 m WFC-INT	2000-02-03	1.3	5N	-	-	600/100	100/10	-

(1) Poor weather conditions. Images not used in the final data.

obtained in the 1998/99 runs and in the OAN 2000 observations, due to adverse meteorological conditions, prevented us from making use of the data collected during those nights. A log of the observations with the total number of frames, exposure times and seeing conditions is given in Table 5.1. Chip specifications were already provided in Table 3.2.

We obtained photometry for a total of 4806 stars in an area of $34' \times 34'$ around NGC 2548, down to a limiting magnitude $V \sim 22$. The area covered by the observations is shown in the finding chart of the cluster (Figure 5.1). Due to the lack of H_β filter at the WFC-INT, it was only possible to measure it at the JKT and CAHA telescopes, thus limiting the spatial coverage with this filter. Only 283 stars have H_β values. Of those only 253 have values of the rest of the Strömgren filters.

Besides long, deep exposures, additional shorter exposures were obtained in order to avoid saturation of the brightest stars. We also took short exposures one degree North from the cluster to use them as a comparison area depicting the field (see last row of Table 5.1 and Section 5.2.1 for more details).

5.1.2 Reduction and transformation to standard system

The reduction of the photometry is explained at length in Chapter 3.1.2 and will not be repeated here. The coefficients of the instrumental-to-standard transforma-

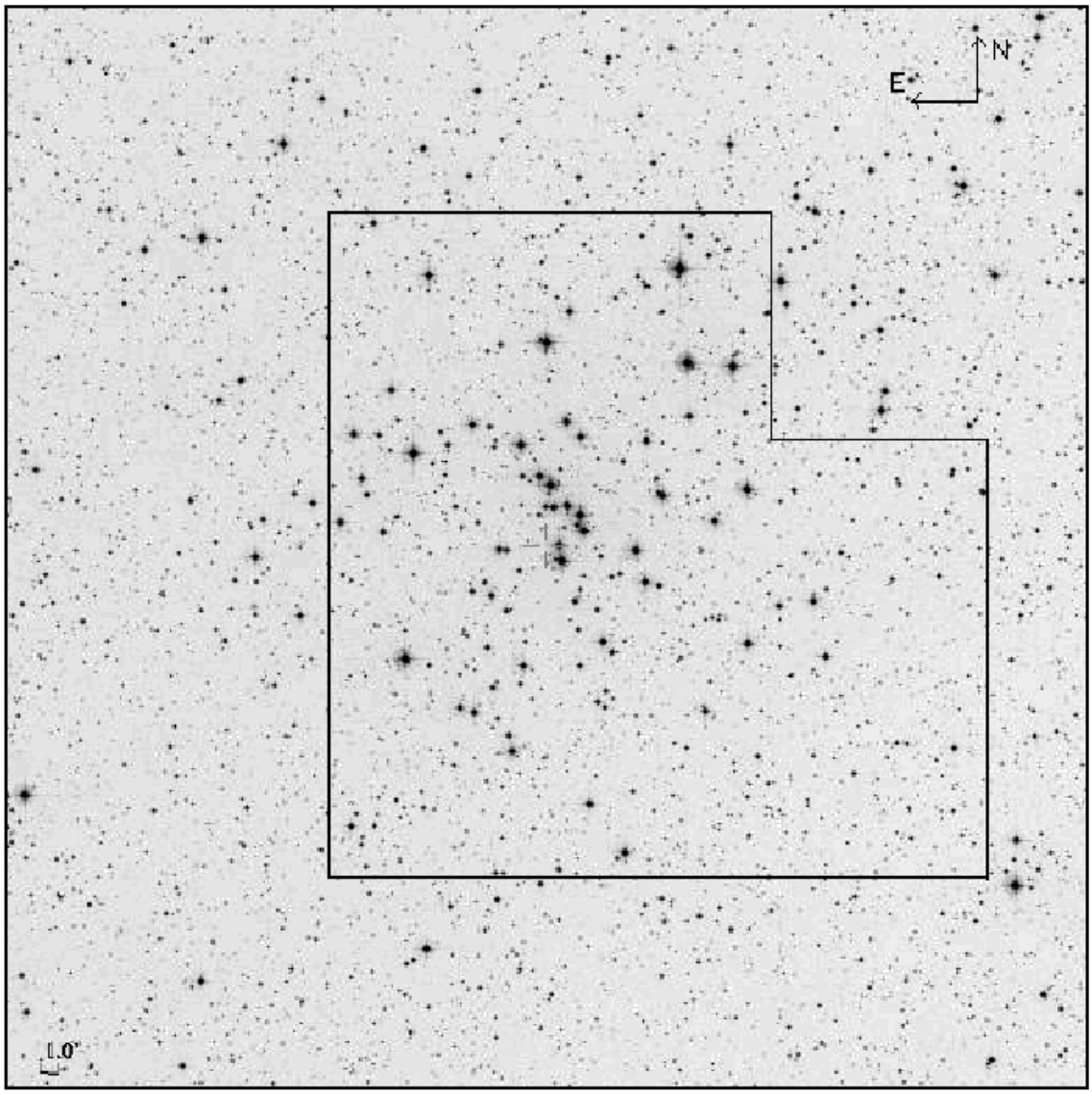

Figure 5.1: Finding chart of the area under study. The covered area is marked in black on an image of a plate (SERC.J—optical B—.DSS1.776-LOW) plotted with Aladin (Bonnarel et al. 2000).

Table 5.2: Number of stars observed (N) and mean internal errors (σ) as a function of apparent visual magnitude.

V range	V		$(b-y)$		m_1		c_1		H_β	
	N	σ	N	σ	N	σ	N	σ	N	σ
8- 9	3	0.019	3	0.028	2	0.016	2	0.002	2	0.017
9-10	19	0.012	19	0.011	19	0.013	16	0.019	5	0.003
10-11	25	0.014	25	0.016	25	0.016	24	0.010	6	0.009
11-12	32	0.012	31	0.013	31	0.018	31	0.016	10	0.030
12-13	45	0.012	43	0.013	43	0.016	43	0.011	12	0.017
13-14	71	0.012	71	0.015	69	0.020	69	0.017	17	0.027
14-15	152	0.012	152	0.023	146	0.029	146	0.030	29	0.016
15-16	260	0.015	260	0.034	259	0.047	251	0.047	42	0.025
16-17	380	0.022	380	0.043	376	0.061	360	0.063	53	0.033
17-18	514	0.030	514	0.035	501	0.043	468	0.043	51	0.036
18-19	639	0.027	639	0.028	592	0.031	477	0.032	8	0.046
19-20	752	0.012	752	0.015	702	0.022	383	0.038		
20-21	859	0.023	859	0.028	662	0.048	160	0.052		
21-22	763	0.049	763	0.063	262	0.089	21	0.082		
22-23	222	0.095	222	0.122	28	0.139				
Total	4736		4733		3717		2451		235	

tion equations were computed by a least squares method using the instrumental magnitudes of the standard stars in NGC 2682 (M 67; Nissen et al. 1987) and their standard magnitudes and colours in the $uvby - H_\beta$ system. The reduction was performed in two steps and following the Equations. (3.1) to (3.6). The mean errors as a function of apparent visual magnitude are given in Table 5.2 for the NGC 2548 stars, and plotted in Figure 5.2.

Table 5.3[2] lists the u, v, b, y, H_β data for all 4806 stars in a region of $34' \times 34'$ around the open cluster NGC 2548 (Figure 5.1). Star centres are given in the frame (x, y) and equatorial ($\alpha_{\rm J2000}$,$\delta_{\rm J2000}$) coordinates. An identification number was assigned to each star following the order of increasing right ascension. Column 1 is the ordinal star number; columns 2 and 3 are $\alpha_{\rm J2000}$ and $\delta_{\rm J2000}$; columns 4 and

[2]Table 5.3 is available in electronic form at the CDS via anonymous ftp to cdsarc.u-strasbg.fr (130.79.128.5) or via `http://cdsweb.u-strasbg.fr/cgi-bin/qcat?J/A+A/437/457/`

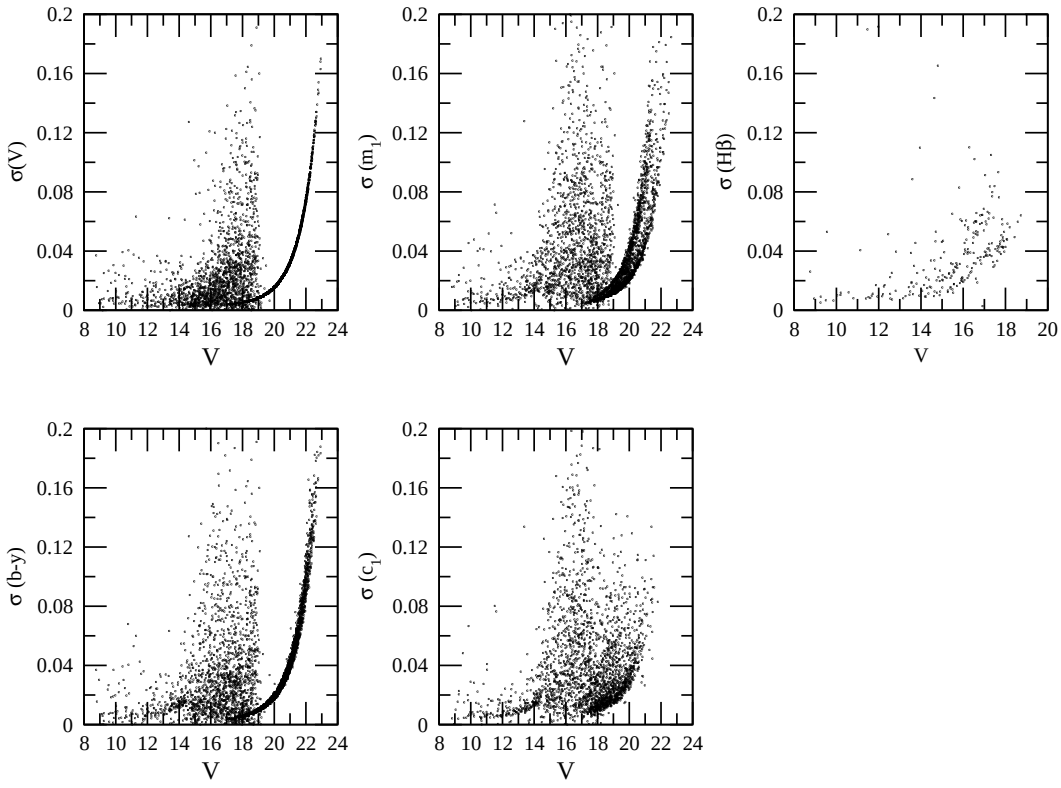

Figure 5.2: Mean internal errors of magnitude and colours as a function of the apparent visual magnitude, V, for all observed stars in the cluster region. The structure in the magnitude dependence is owed to the mosaic of images from different nights and different telescopes having different limiting magnitude.

5 are the respective x, y coordinates in arcmin; columns 6 and 7 are the $(b-y)$ and its error, 8 and 9 the V magnitude and its error, 10 and 11 the m_1 and its error, 12 and 13 the c_1 and its error, and 14 and 15 the H_β and its error. In column 16, stars considered candidate members (see Section 5.2.2.) are labelled 'M', while those classified as non-members show the label 'NM'.

The cross-identification of stars in common with the astrometry (Chapter 4), BDA (`http://obswww.unige.ch/WEBDA`), Hipparcos (ESA, 1997), Tycho-2 (Høg et al. 2000) and USNO-2 (Monet et al. 1998) catalogues is provided in Table 5.4[3].

5.1.3 Comparison with previous photometry

Only three stars in the NGC 2548 area have been previously studied using Strömgren photometry (BDA 0366, 1560, 2156). Unfortunately, none of them is inside the area covered by our photometry. Only one of them (BDA 1560) is considered a cluster member from our astrometry and will be studied in Section 5.3.2.

The V magnitude derived from the y filter can be compared with the published broadband data. There are 30 stars in common with Pesch (1961). The corresponding mean difference in V, in the sense ours minus Pesch' is -0.01 ± 0.03.

Transformations between $B-V$ and $b-y$ from several authors (see Moro & Munari, 2000) fails to cover the whole range under study. We can find a linear relation between the two indices: $B-V = (1.632\pm0.031)(b-y) - (0.038 \pm 0.010)$, N=30. The standard deviation of the residuals about the mean relation is 0.048, where the typical uncertainty in $B-V$ is 0.02 and in $b-y$ is 0.016.

5.2 Colour-Magnitude diagrams

We use the V vs $(v-y)$ colour-magnitude diagram for our study. The colour-magnitude diagram based on this colour index defines the main-sequence of a cluster significantly better than the traditional V vs $(b-y)$ diagram (Figure 5.3 left and

[3]Table 5.4 is available in electronic form at the CDS via anonymous ftp to cdsarc.u-strasbg.fr (130.79.128.5) or via `http://cdsweb.u-strasbg.fr/cgi-bin/qcat?J/A+A/437/457/`

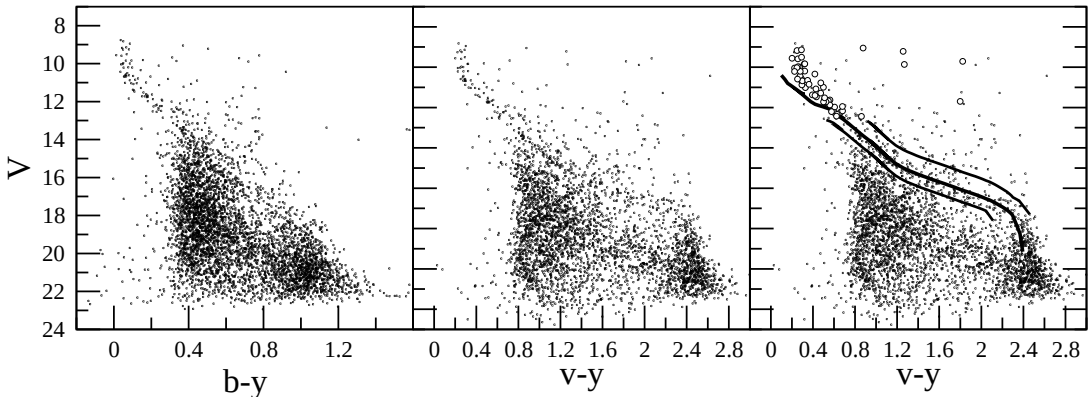

Figure 5.3: The colour-magnitude diagram of the NGC 2548 area. Empty circles in the right figure are the astrometric members of Chapter 4. Thick line is a shifted ZAMS, with the chosen margin for candidate members ($V+0.5$,$V-1$) in thin lines. See text for details.

centre). The colour-magnitude diagram of all the stars in the area displays a fairly well defined main sequence.

5.2.1 Non-parametric approach in the photometric plane

Following the same method as explained in Section 3.2.1, we try to use the non-parametric technique for membership segregation in the photometric plane. The colour-magnitude diagram of the area shows an outstanding main sequence related to the cluster. On the contrary, the comparison field, located one degree North from the cluster, seems reasonably clean of cluster members.

We do not need to define different areas for the cluster and the field as both have the same size. However, as the comparison field is not as deep as the cluster area, we need to fix a magnitude limit. We made different tries changing this limit as well as posing also limits on $b-y$, but none seemed to work well. One of those tries (with $V_{\rm lim}=18$) can be seen in Figure 5.4. As we have seen in Section 3.2.1, the different distribution of errors makes the reliability of this result dubious.

To check the problem related to the dispersion of the errors structure we tried with Galaxy models from Besançon (Robin et al. 2003). Three of those fields with different error models can be seen in Fig 5.5. However, the same problem with the

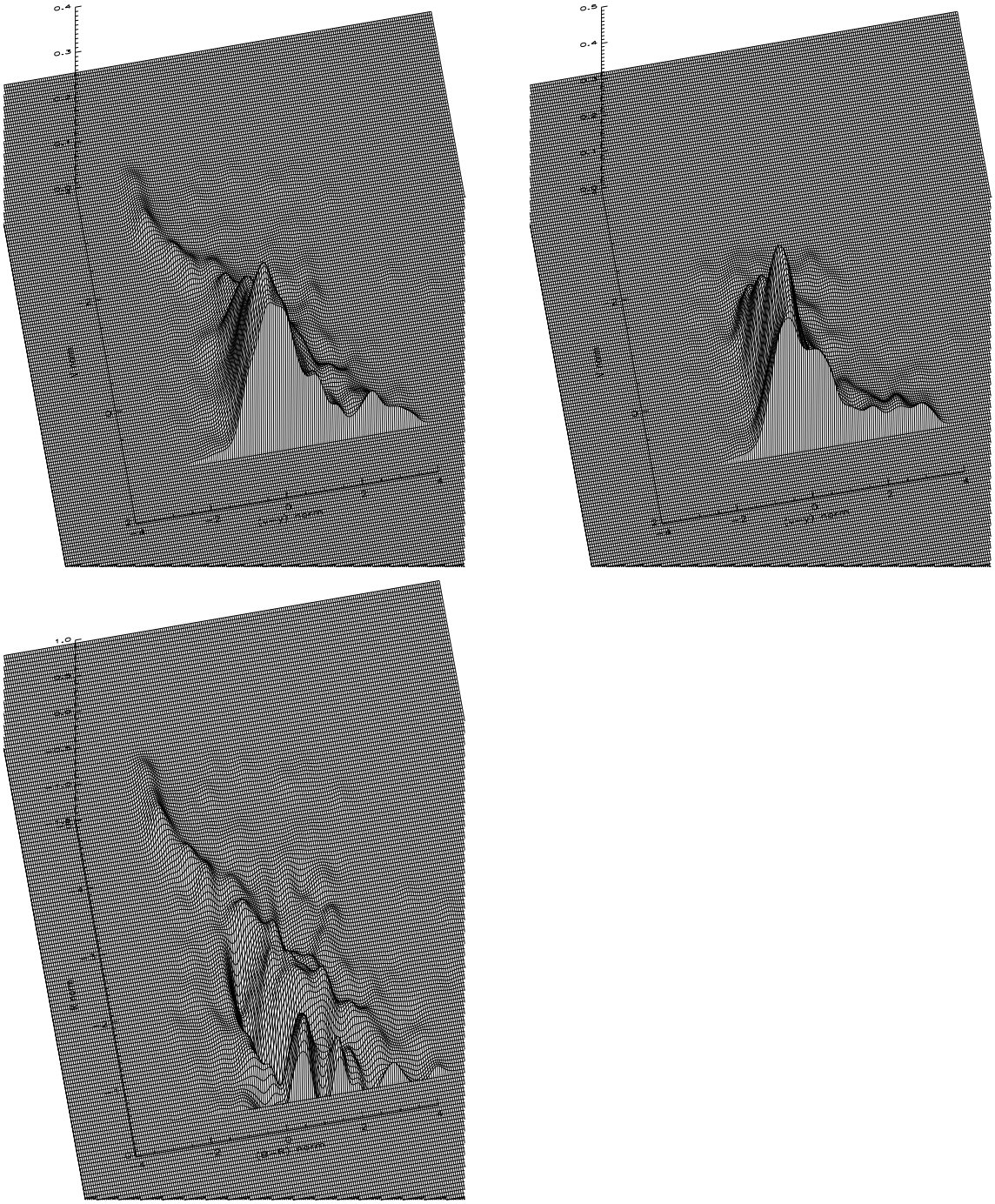

Figure 5.4: The photometric empirical PDF's. Top left: ψ^p_{c+f} (mixed sample). Top right:ψ^p_f (field population). Bottom: ψ^p_c (non-field). The view angle is chosen to highlight the different internal structure induced into the data by the differences in the distribution of errors.

errors influence in the PDF's appeared and discouraged us from using this technique with photometric data. Therefore, we made use of the photometric information in the classical way, as explained in the next section.

5.2.2 Selection of candidate member stars

Our photometric measurements help to reduce the possible field contamination in the proper motion membership among bright stars, as well as to enlarge the selection of members towards faint magnitudes, as already seen for NGC 1817 in Section 3.2.2. Among those astrometric member stars with photometric measurements, we find one star that is not compatible with the sequence of the cluster outlined in the colour-magnitude diagram. Our astrometric segregation of member stars has a limiting magnitude of $V \sim 13$. From this point down to $V = 18$ we construct a ridge line following a fitting of the observational ZAMS (Crawford 1975, 1978, 1979, Hilditch et al. 1983, Olsen 1984) in the $(V, v-y)$ diagram. A selection of stars based on the distance to this ridge line is then made. The chosen margin for candidates includes all the stars between $V + 0.5$ and $V - 1$ from the ridge line, as shown in the right panel of Figure 5.3. The margins were chosen to account for observational errors and the presence of multiple stars.

This preliminary photometric selection is refined in the colour-colour diagrams (Figure 5.6) with the help of the standard relations from the same authors. A final selection of 331 stars is plotted as empty circles in the $[m_1] - [c_1]$, $m_1 - (b-y)$, $c_1 - (b-y)$ and $[c_1] - H_\beta$ diagrams.

5.3 Fundamental parameters of the cluster

The stars selected as possible cluster members were classified into photometric regions and their physical parameters were determined as explained in Section 3.3 for each of the photometric regions of the HR diagram. Absolute magnitude, effective temperature and gravity as well as the corresponding reddening, distance modulus, metallicity and raw spectral type and luminosity class are calculated for each star. Typical errors are 0.25 mag in M_V, 0.15 dex in [Fe/H], 270 K in $T_{\rm eff}$, 0.18 dex in $\log g$ and 0.015 mag in $E(b-y)$.

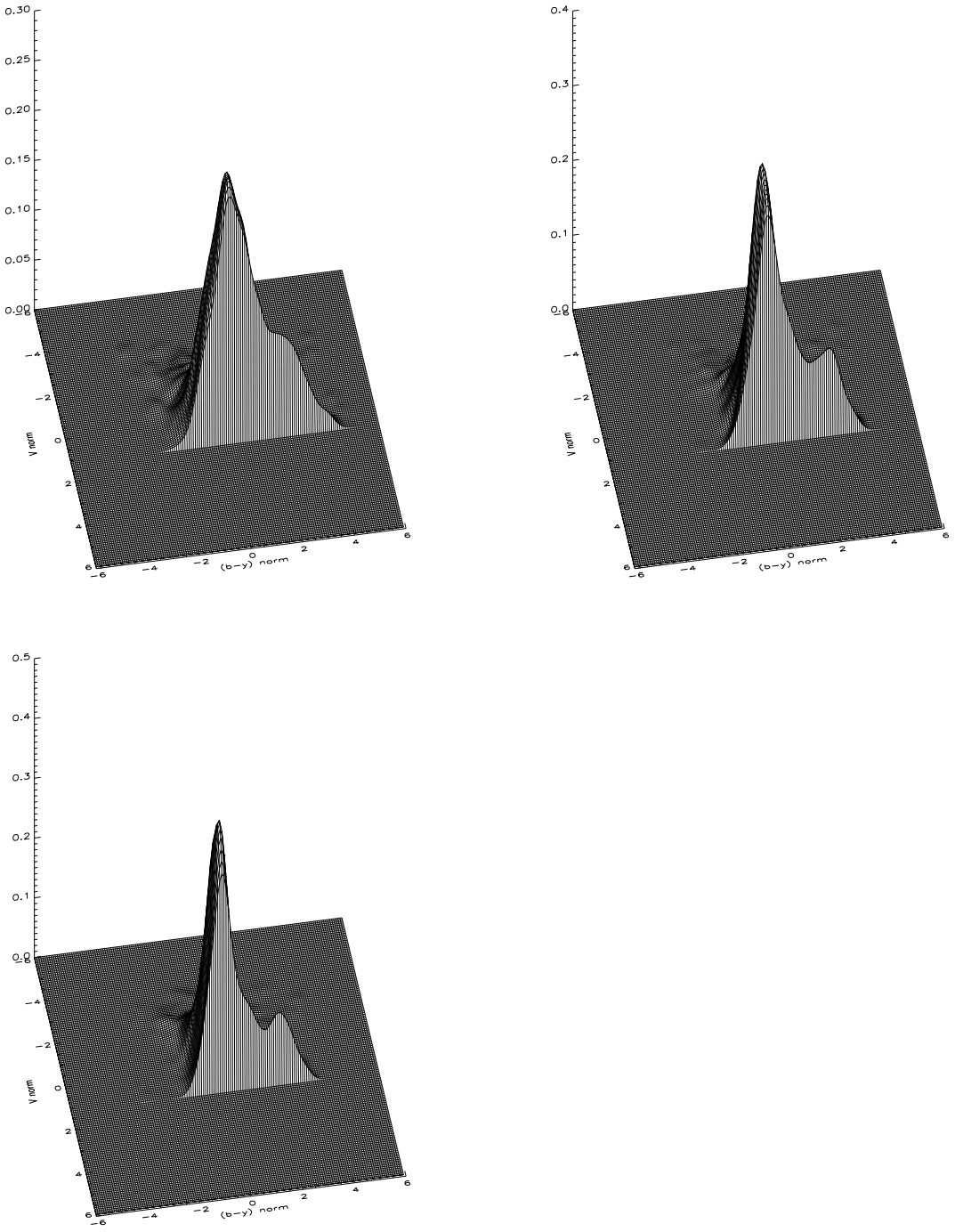

Figure 5.5: The photometric empirical PDF's from the Besançon model (Robin et al. 2003) with three different amounts for the error values.

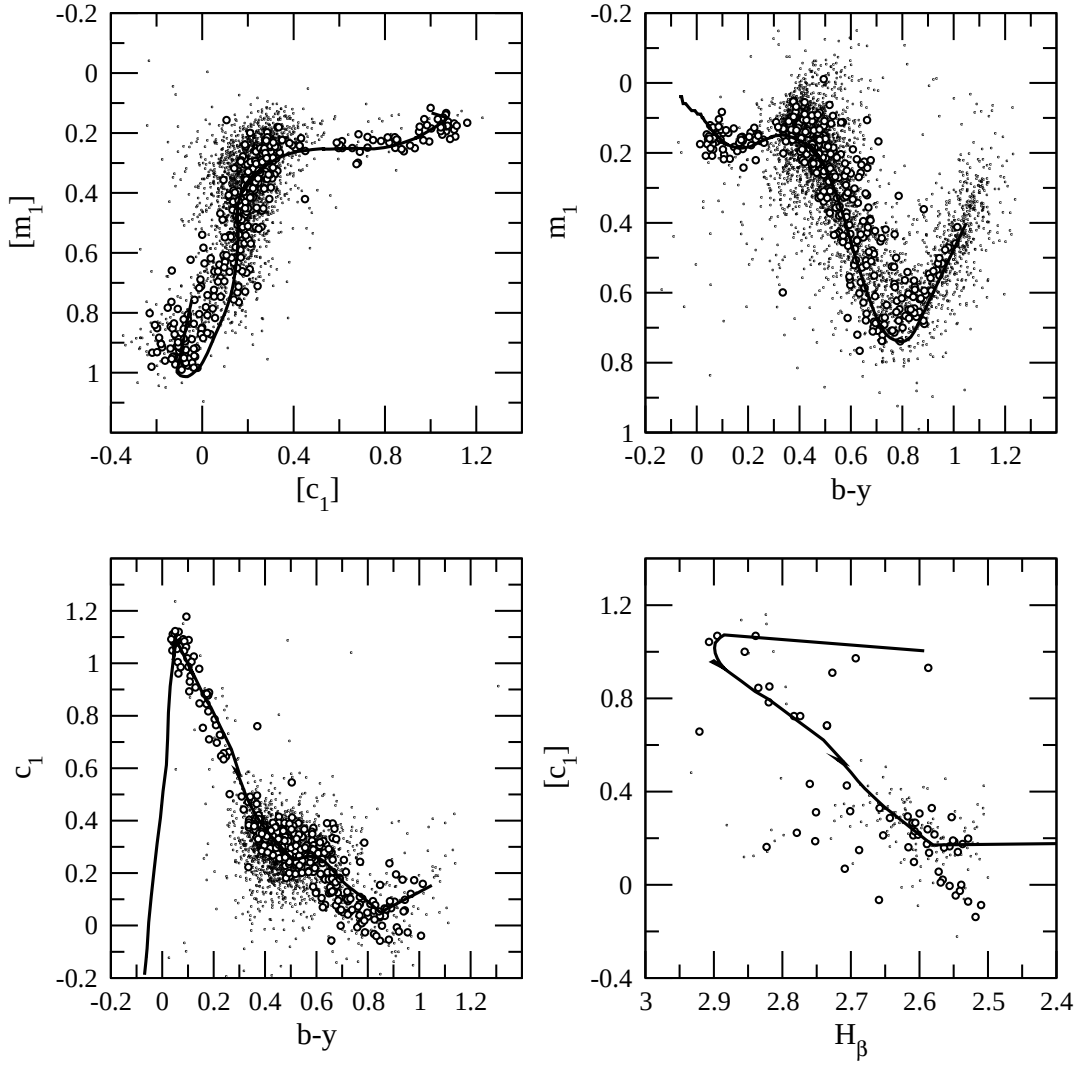

Figure 5.6: The colour-colour diagrams of NGC 2548. Empty circles denote candidate members of NGC 2548, chosen with astrometric and non-astrometric criteria as explained in Section 5.2.2. The thick line is the standard relation shifted by $E(b-y) = 0.06$ when necessary.

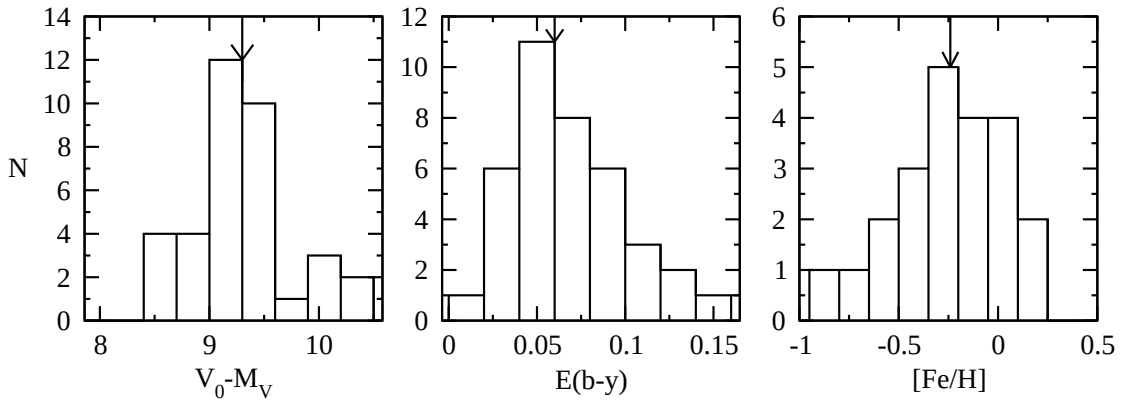

Figure 5.7: The histograms of the distance modulus, reddening and metallicity of the selected member stars of NGC 2548 with H_β measuremenets. The arrows indicate the mean values adopted for the cluster.

The fundamental parameters of NGC 2548 found in Chapters 4 and the present one are resumed in Table 5.7.

5.3.1 Distance, reddening and metallicity

Only 62 stars among the 331 candidate members have H_β measurements. Thus the computation of physical parameters is only possible for that subset. The results are shown in Figure 5.7. Excluding peculiar stars and those with inconsistencies in their photometric indices and applying an average with a 2σ clipping to that subset, 39 stars remain. We found a reddening value of $E(b-y) = 0.06 \pm 0.03$ (corresponding to $E(B-V) = 0.08$) and a distance modulus of $V_0 - M_V = 9.3 \pm 0.5$ (725 pc, i.e. about 200 pc above the galactic plane). Metallicity is better calculated studying only the 26 F and G stars in our sample following Masana (1994). We found a value of [Fe/H] $= -0.24 \pm 0.27$.

5.3.2 Red giants

To complete our spatial photometric limit, we have examined the bibliography in search of bright stars in the area of NGC 2548. We have found only one compatible with being an astrometric member of the cluster: the brightest star (BDA 1560), that was inside our field but saturated in our data. We therefore took its values

Table 5.5: Red giants in NGC 2548 region, with their membership. The first five are from the BDA list of Red Giants. Three of them are known spectroscopic binaries.

Phot. Id.	BDA	$(b-y)$	V	P_P	P_{NP}	M/NM	
1006	870	0.670±0.0185	9.712±0.0185	0.07	0.84	M?	
2556	1218	0.335±0.0370	9.862±0.0305	0.83	0.85	M	
2732	1260	0.370±0.0002	9.050±0.0047	0.97	0.84	M	SB
2894	1296	0.504±0.0004	9.215±0.0023	0.94	0.86	M	SB
(1)	1560	0.724±0.0020	8.199±0.0060	0.88	0.84	M	SB
3971	1521	0.312±0.0079	9.671±0.0081	0.00	0.00	NM	
4557	1616	0.719±0.0045	9.890±0.0045	0.00	0.00	NM	
2645	1241	0.777±0.0072	9.565±0.0072	0.81	0.66	NM?	

(1) Photometry taken from Olsen (1993)

from Olsen (1993). The stars in the red giant region are detailed in Table 5.5. Three of them are known spectroscopic binaries. We are cautious about our values of star BDA 1218, as the known values of V are 9.64 (Pesch 1961) and 9.63 (Oja 1976), about 0.2 mag brighter than our values. Star BDA 870 was considered to be an astrometric non-member by Ebbinghausen (1939) and in Chapter 4, while Clariá (1985) studied its weak CN peculiarity and opened the possibility of a cluster member with peculiar composition and proper motion. Star BDA 1241 is considered to be a cluster member in Chapter 4.

5.3.3 Age

The recent publication by Clem et al. (2004) of empirically constrained colour-temperature relations in the Strömgren system enables an isochrone fitting to our results. The best fit is found for the recent Pietrinferni et al. (2004) tracks. Figure 5.8 shows isochrones of [Fe/H] $= -0.25$ for canonical models (right panel) and for models with overshooting (left panel). Taking into account the number of stars before and after the MS hook, we found a best fit for models with overshooting. The estimated age is of 400±100 Myr ($\log t = 8.6$). Using a different set of tracks by Schaller et al. (1992) we also found agreement with a best estimation of the age of $\log t = 8.6 \pm 0.1$. Neither Pietrinferni et al. (2004) nor Schaller et al. (1992) isochrones provide a perfect fit to the giant members. Similar discrepancies were found by Lapasset et al. (2000) studying the intermediate-age cluster NGC 2539.

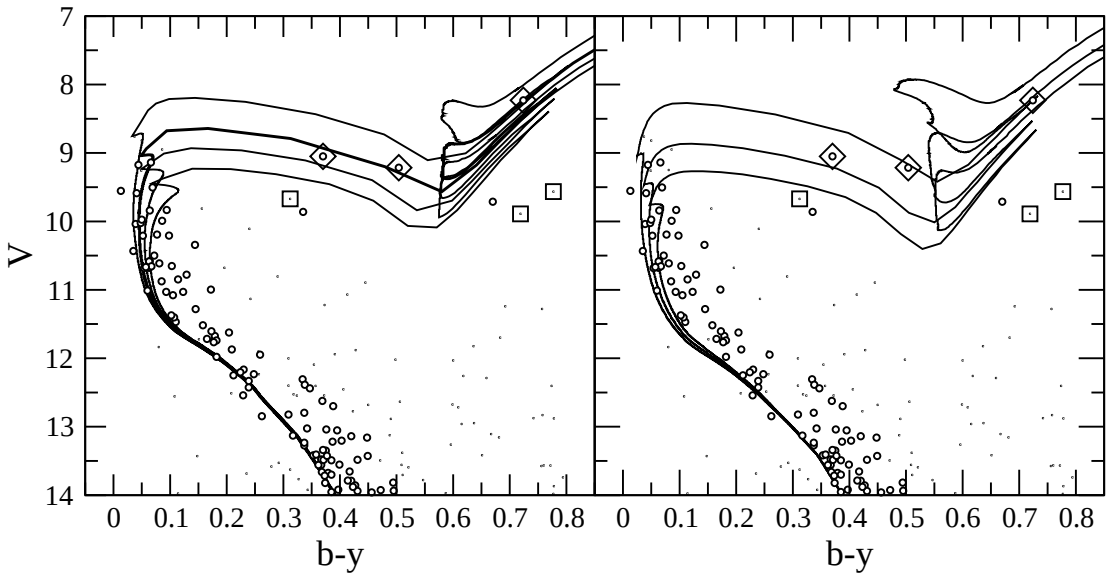

Figure 5.8: Isochrones from Pietrinferni et al. (2004) for scaled solar models of [Fe/H] $= -0.25$ and ages of 300, 400, 500, 600 Myr for models with overshooting (left panel) and 200, 300, 400 Myr for canonical models (right panel). Empty circles are candidate members. Red giants are analysed in detail (see text): diamonds are spectroscopic binaries, squares are astrometric non-members. The adopted reddening and distance modulus are $E(b-y) = 0.06$ and $V_0 - M_V = 9.3$.

5.3.4 Dimension and mass

We have found 118 members out of a sample of 501 stars (24%) in an area of 1.°6 × 1.°6 covered by our astrometry study with magnitude limit of $V_{\rm lim} \sim 13$. We calculate the half-sample radius from this astrometry selection. The first step is to calculate the real centre of the cluster from the list of members. A radius of $r_{\rm h} = 14.38'$ is found. Taking the calculated distance of 725 pc, it means a half-sample radius of 3.0 pc. From the photometric study we cover a smaller area ($34' \times 34'$) but to a much deeper magnitude ($V_{\rm lim} = 18$), and found 331 members out of 1501 (22%).

The total stellar density was taken from the central density of the cluster: $\sigma = 3.06$ stars pc^{-3} which corresponds to a mean space density of $\rho = 3.79$ M$_\odot$ pc^{-3}. We can calculate the total mass of the cluster only as a lower limit, due to our magnitude limit and spatial coverage. As for NGC 1817, the isochrone computed by Pietrinferni et al. (2004) has been used to derive individual masses of the cluster members and to calculate a minimum total mass, without taking into account the binaries contribution. For NGC 2548 the total mass is greater than 370 M$_\odot$.

5.3.5 Comparison with other studies

Our results are consistent with previous studies. Pesch (1961) gives an $E(B-V) = 0.04 \pm 0.05$ and a distance of 630 pc from UBV photoelectric observations of 30 stars. Clariá (1985) studied DDO photometry of 5 giant stars and gives a value of $E(B-V) = 0.06$ and a distance of 530 pc. Twarog et al. (1997) revised those values and gave an $E(B-V) = 0.05$, a distance of 590 pc and [Fe/H] = 0.08 from 3 stars. Harris (1976) gives a value of $\log t = 8.28$ from an analysis of nine stars. Høg & Flynn (1998) give [Fe/H] = −0.13, $E(B-V) = 0.04$ and $\log t = 8.50$ from DDO photometry of three giants. Rider et al. (2004) fix a value $E(B-V) = 0.03$ from the bibliography and give values of distance 700 pc, $[Z/{\rm Z}_\odot] = 0.0$ and an age of 400 Myr by isochrone fitting to $u'g'r'i'z'$ photometry. The recent study by Wu et al. (2005) gives a slightly larger distance (780 pc) and a lower age (0.32 Gyr) also fitting isochrones with $E(B-V) = 0.04$ and solar metallicity. Results from studies based on giant stars give distances smaller than the more complete, recent results. A summary of this information is given in Table 5.6 for clarity.

Table 5.6: Comparison of the physical parameters of the cluster with results from other authors. See the text for detailed information of the assumptions made in each case.

Reference	$E(B-V)$	[Fe/H]	$\log t$	Distance	Comments
	mag	dex		pc	
This work	0.08	-0.24 ± 0.27	8.6 ± 0.1	725	
Wu et al. (2005)	0.04	0.0	8.51	780	Isochrone fit
Rider et al. (2004)		0.0	8.60	700	Isochrone fit
Høg & Flynn (1998)	0.04	-0.13	8.50		DDO Phot. 3 stars
Harris (1976)			8.28		Phot. 9 stars
Twarog et al. (1997)	0.05	0.08		590	DDO Phot. 3 stars
Clariá (1985)	0.06	0.1		530	DDO Phot. 5 stars
Pesch (1961)	0.04			630	UBV Photoelectric 30 stars

Table 5.7: Fundamental parameters of NGC 2548

Identifiers	NGC 2548, M 48, C 0811-056
Position	$\alpha_{2000} = 8^{\rm h}13^{\rm m}48^{\rm s}$, $\delta_{2000} = -5°48'$
	$l = 227\overset{\circ}{.}93$, $b = +15\overset{\circ}{.}39$
	in Hydra
Distance	$V_0 - M_V = 9.3 \pm 0.5$
	$d = 725$ pc
	$z = 194$ pc
Half-sample radius	$r_{\rm h} = 14.38'$ (3 pc)
Proper motion	$\mu_\alpha \cos\delta = -1.10 \pm 0.08$ mas yr^{-1}
	$\mu_\delta = 2.09 \pm 0.08$ mas yr^{-1}
Reddening	$E(b-y) = 0.06 \pm 0.03$
	$E(B-V) = 0.08 \pm 0.05$
Age	$\log t = 8.6 \pm 0.1$
	$t = 400 \pm 100$ Myr
Metallicity	[Fe/H] $= -0.24 \pm 0.27$
Membership	N(M) = 118 ($V_{\rm lim} = 13$) in an area of $1\overset{\circ}{.}6 \times 1\overset{\circ}{.}6$
	N(M) = 331 ($V_{\rm lim} = 18$) in an area of $34' \times 34'$
Giants	N(RG) = 5
(in an area of $34' \times 34'$)	N(RG-SB) = 3
Central stellar density	$\sigma = 3.06$ stars pc^{-3}
	$\rho = 3.79$ M$_\odot$ pc^{-3}
Cluster Mass	$M_{\rm tot} > 370$ M$_\odot$